The 8th European Congress on Computational Methods in Applied Sciences and Engineering
ECCOMAS Congress 2022
5-–9 June 2022, Oslo, Norway

A COROTATIONAL MIXED FLAT SHELL FINITE ELEMENT FOR THE EFFICIENT GEOMETRICALLY NONLINEAR ANALYSIS OF LAMINATED COMPOSITE STRUCTURES

Francesco S. Liguori [1] **and Antonio Madeo** [1]

[1] DIMES, University of Calabria, Ponte P. Bucci Cubo 42b, 87036 Rende (Cosenza), Italy

Key words: Laminated composite shell, corotational formulation, geometrically nonlinear analysis, mixed shell element, Hellinger-Reissner variational principle, hybrid-Trefftz method.

Abstract. A corotational mixed flat shell element for the geometrically nonlinear analysis of laminated composite structures is presented. The stress interpolation is derived from the linear elastic solution for symmetric composite materials.Displacement and rotation fields are only assumed along the contour of the element. As such, all the operators are efficiently obtained through analytical contour integration. The geometrical nonlinearity is introduced by means of a corotational formulation. The proposed finite element, named MISS-4c, proves to be locking free and shows no rank defectiveness. A multimodal Koiter's algorithm is used to obtain the initial postbuckling response. Results show good accuracy and high convergence rate in the geometrically nonlinear analysis of composite shell structures.

1 INTRODUCTION

The geometrically nonlinear analysis of composite shell structures attracts nowadays the interests of many fields. Much effort has been invested to develop high-performing materials and breakthrough technologies that allow to reduce weight in structural shell components. Accordingly, optimal design strategies have been presented to exploit the whole potential that new technologies offer [23, 18]. One of the key aspects in such procedures is the efficiency and robustness of geometrically nonlinear analyses. As such, many recent proposals move in this direction. This goal is reached, for instance, through the use of efficient solution algorithms, like in Koiter-like methods [14, 9] Conversely, the reduction of the discrete variables is pursued, among the others, by the isogeometric formulations [16, 15] that take advantage from the high continuity of interpolation functions, and by high-performing Finite Elements (FE) [22, 5]. Within this last group of FE, interesting results have been obtained by mixed formulations that assume both displacement and stresses fields as primary variables [6]. In such FE, the selection of the interpolation function for the stress field is of paramount concern. The minimum number of stress parameters is equal to the number of kinematical parameters minus the number of rigid body motions. If the minimum number of stress parameter is adopted, the element is defined as isostatic and the stress field is uniquely defined by the equilibrium equations of the element and it has been previously shown how this guarantees the best FE response. Madeo et al. [20] proposed a simple four node mixed isostatic FE in which the stress fields a-priory satisfy equilibrium equations for zero bulk loads, obtaining good convergence properties in the linear-elastic case.

The element is afterwards extended to buckling and postbuckling analyses using a corotational (CR) formulation [2].

Since the first works on the topic [24], the corotational (CR) formulation has shown a great potential in the description of geometrically nonlinearity for both continuum and discrete models. The main context of application is that of large deformations (large displacements and rotations) and small strains with assumed linear-elastic constitutive equations. Within this framework, the CR formulation allows the decomposition of the large deformation into two contributions, namely the small strains and the rigid body motions [8]. Using an appropriate CR reference system, the rigid body motion can be filtered, thereby obtaining a simplified description of small strains. This means that linear equations can be used in the CR reference system. In this way all models (continuum or discrete) available in the linear context can be reused to obtain the corresponding nonlinear ones [10]. Due to its attractive features, the CR formulation has been extensively employed through the years. Recently, it has been applied to 3D beams [12], Generalised Beam Theory (GBT) [26], plate/shell models [3], solid-shell formulations [5].

An interesting technique for developing efficient mixed FE is the hybrid-Trefftz method [13]. It is based on assumed stresses that a-priori satisfy both equilibrium equations for zero bulk loads and compatibility equations in the linear-elastic case and displacement fields assumed along the element contour only [4]. Based on this technique, a mixed FE for the linear-elastic analysis of isotropic shell structures has been recently proposed [21]. This element, named MISS-8, is characterised by accuracy for coarse meshes, high convergence rate and insensitivity to mesh distortion. However, the extension of hybrid-Trefftz FE to structures made of composite materials is not straightforward. The elastic matrix, in fact, has influence on the compatibility equations and, therefore, on the interpolation of the stress fields.

In this work, a novel mixed FE for the geometrically nonlinear analysis of composite shell structures is proposed. The element is derived from the Hellinger-Reissner variational principle in which both stress and displacement fields are assumed as primary unknowns. Inspired by the hybrid-Trefftz method, the stress fields a-priori satisfy both equilibrium for zero bulk loads and compatibility equations. In particular, the stress fields are derived for composite materials characterised by symmetric stacking sequences. The element geometry is flat and has 24 kinematical degrees of freedom, located at the four vertices. In particular, each node has three displacements and three rotations, including drilling. The element is isostatic and, therefore, the number of stress parameters is 18.

Due to the nature of the stress interpolation, it is possible to interpolate displacements and rotations only along the element contour. Along each side, the membrane displacements and the drilling rotations are handled a la Allman [1], whereas the flexural displacements and rotations are coupled by a linked interpolation [7]. A cubic, incompatible out-of-plane displacement is introduced. The element matrices are integrated analytically using contour integration. No rank defectiveness and spurious energy modes are detected. The element, formulated in the linear-elastic case, is employed for the solution of the geometrically nonlinear problem through a CR formulation. Koiter's asymptotic algorithm is used to obtain the buckling and initial postbuckling behaviour [11].

Based on the main features introduced above, the element is named MISS-4c (Mixed, Isostatic, Self-equilibrated Stress for Composite). In MISS-4c, the use of assumed stress fields that satisfy equilibrium and compatibility equations is extended to composite structures. Therefore, the

coefficients of the elastic matrix, obtained by means of the First Order Shear Deformation Theory (FSDT), influence the stress interpolation functions. Additionally, the hybrid-Trefftz method, commonly used in the linear-elastic case, is successfully adopted for geometrically nonlinear analyses of shell structures. Results show that MISS-4c exhibits good convergence properties in the linear solution, in the buckling analysis and in the evaluation of the initial postbuckling behaviour.

2 MIXED VARIATIONAL FORMULATION AND LINEAR FINITE ELEMENT MODEL

2.1 Hellinger-Reissner variational formulation

MISS-4c is developed from the Hellinger-Reissner functional, which is

$$\Pi[\boldsymbol{t},\boldsymbol{d}] = \Phi[\boldsymbol{t},\boldsymbol{d}] - \mathrm{W}[\boldsymbol{t},\boldsymbol{d}], \tag{1}$$

where $\Pi[\boldsymbol{t},\boldsymbol{d}]$ is the total potential energy, $\Phi[\boldsymbol{t},\boldsymbol{d}]$ is the mixed strain energy expressed in terms of stress resultants $\boldsymbol{t}$ and generalised displacements $\boldsymbol{d}$, while $\mathrm{W}[\boldsymbol{t},\boldsymbol{d}]$ is the work done by external loads. The mixed strain energy for flat shells is expressed as

$$\Phi[\boldsymbol{t},\boldsymbol{d}] = \Phi_d[\boldsymbol{t},\boldsymbol{d}] - \Phi_c[\boldsymbol{t}], \tag{2}$$

where the strain work $\Phi_d[\boldsymbol{t},\boldsymbol{d}]$ and the complementary strain energy $\Phi_c[\boldsymbol{t}]$ are defined as

$$\Phi_d[\boldsymbol{t},\boldsymbol{d}] = \int_\Omega \left(\boldsymbol{t}^T \boldsymbol{e}[\boldsymbol{d}]\right) \mathrm{d}\Omega \quad , \quad \Phi_c[\boldsymbol{t}] = \frac{1}{2}\int_\Omega \left(\boldsymbol{t}^T \boldsymbol{E}^{-1}\boldsymbol{t}\right) \mathrm{d}\Omega, \tag{3}$$

being Ω the two-dimensional structural domain. The stress resultants and the generalised strains are expressed as

$$\boldsymbol{t} = \begin{bmatrix} \boldsymbol{t}_m \\ \boldsymbol{t}_f \end{bmatrix} \quad , \quad \boldsymbol{d} = \begin{bmatrix} \boldsymbol{d}_m \\ \boldsymbol{d}_f \end{bmatrix}, \tag{4}$$

where subscripts m and f indicate the membrane and out-of-plane quantities, respectively.

Afterwards, the compatibility equations are obtained as $\boldsymbol{e}[\boldsymbol{d}] = \boldsymbol{Q}\boldsymbol{d}$, where $\boldsymbol{Q}$ is the differential operator

If the structure is subject to bulk loads $\bar{\boldsymbol{q}}$, contour distortions $\bar{\boldsymbol{e}}$ and tractions $\bar{\mathbf{f}}$, the external work $\mathrm{W}[\boldsymbol{t},\boldsymbol{d}]$ becomes

$$\mathrm{W} = \int_\Omega \boldsymbol{d}^T \bar{\boldsymbol{q}} \,\mathrm{d}\Gamma + \int_\Omega \boldsymbol{t}^T \bar{\boldsymbol{e}} \,\mathrm{d}\Gamma + \int_\Gamma \boldsymbol{d}^T \bar{\mathbf{f}} \,\mathrm{d}\Gamma. \tag{5}$$

where Γ is the contour of Ω. If $\boldsymbol{t}$ satisfies the equilibrium equations with zero bulk loads, it follows that

$$\boldsymbol{Q}_m^T \boldsymbol{t}_m = \mathbf{0} \quad , \quad \boldsymbol{Q}_b^T \boldsymbol{t}_b - \hat{\boldsymbol{I}}\boldsymbol{t}_s = \mathbf{0} \quad , \quad \boldsymbol{Q}_s^T \boldsymbol{t}_s = \mathbf{0}. \tag{6}$$

In light of this, the following identity holds

$$\int_\Omega \boldsymbol{t}^T \boldsymbol{Q}\boldsymbol{d} \,\mathrm{d}\Omega = \int_\Gamma \boldsymbol{t}^T \boldsymbol{N}_\Gamma \boldsymbol{d} \,\mathrm{d}\Gamma, \tag{7}$$

where $\boldsymbol{N}_\Gamma$ is the matrix collecting the components of the unit outward normal to the contour $\boldsymbol{n} = [n_x, n_y]^T$, whose expression is given elsewhere [17] If $\boldsymbol{t}$ satisfies also the compatibility equations, then it represents a possible solution $\boldsymbol{d}_t$ of the elastic displacement field, that is

$$\boldsymbol{t} = \boldsymbol{E}\boldsymbol{Q}\boldsymbol{d}_t. \tag{8}$$

Therefore, it is possible to write the following identity

$$\int_\Omega \boldsymbol{t}^T \boldsymbol{E}^{-1} \boldsymbol{t} \mathrm{d}\Omega = \int_\Gamma \boldsymbol{t}^T \boldsymbol{N}_\Gamma \boldsymbol{d}_t \, \mathrm{d}\Gamma. \tag{9}$$

By recalling Eqs. (7) and (9), the mixed strain energy is conveniently evaluated by line integration along Γ.

2.2 Mixed FE: stress and displacement fields interpolations

Stress and displacement fields are approximated separately within the FE. By denoting with the subscript e the generic element, the stress resultants are interpolated as

$$\boldsymbol{t} = \boldsymbol{B}\boldsymbol{t}_e, \quad \begin{bmatrix} \boldsymbol{t}_m \\ \boldsymbol{t}_f \end{bmatrix} = \begin{bmatrix} \boldsymbol{B}_m & \cdot \\ \cdot & \boldsymbol{B}_f \end{bmatrix} \begin{bmatrix} \boldsymbol{\beta}_m \\ \boldsymbol{\beta}_f \end{bmatrix}, \tag{10}$$

where the interpolation matrices $\boldsymbol{B}_m$ and $\boldsymbol{B}_f$ collect the stress modes assumed for the membrane and the flexural generalised stresses, respectively. Additionally, the interpolation parameters for the membrane and flexural stress fields are collected in $\boldsymbol{\beta}_m$ and $\boldsymbol{\beta}_f$, respectively.

To interpolate the displacement fields it is assumed that

$$\boldsymbol{d} = \boldsymbol{D}\boldsymbol{d}_e, \quad \begin{bmatrix} \boldsymbol{d}_m \\ \boldsymbol{d}_f \end{bmatrix} = \begin{bmatrix} \boldsymbol{D}_m & \cdot \\ \cdot & \boldsymbol{D}_f \end{bmatrix} \begin{bmatrix} \boldsymbol{d}_{me} \\ \boldsymbol{d}_{fe} \end{bmatrix}, \tag{11}$$

where the matrices $\boldsymbol{D}_m$ and $\boldsymbol{D}_f$ collect the shape functions for the in-plane and out-of-plane displacements, respectively. The vectors $\boldsymbol{d}_{me}$ and $\boldsymbol{d}_{fe}$ collect the interpolation parameters for the in-plane and out-of-plane displacements, respectively. As a result, the mixed strain energy of the element is evaluated by substituting Eqs. (10) and (11) into (2) and integrating over Ω_e, thereby obtaining

$$\Phi_e[\boldsymbol{t}_e, \boldsymbol{d}_e] = \boldsymbol{t}_e^T \boldsymbol{Q}_e \boldsymbol{d}_e - \frac{1}{2} \boldsymbol{t}_e^T \boldsymbol{H}_e \boldsymbol{t}_e, \quad \begin{cases} \boldsymbol{Q}_e = \displaystyle\int_{\Omega_e} \left\{ \boldsymbol{B}^T \boldsymbol{Q} \boldsymbol{D} \right\} \mathrm{d}\Omega \\ \boldsymbol{H}_e = \displaystyle\int_{\Omega_e} \left\{ \boldsymbol{B}^T \boldsymbol{E}^{-1} \boldsymbol{B} \right\} \mathrm{d}\Omega \end{cases}, \tag{12}$$

where $\boldsymbol{Q}_e$ and $\boldsymbol{H}_e$ are the compatibility and compliance matrices of the generic element, respectively. In a similar way one can evaluate the element force vector $\boldsymbol{f}_e$ from the expression of the external work W.

If one assumes that $\boldsymbol{t}$ satisfies the equilibrium equations with zero bulk loads, the matrix $\boldsymbol{Q}_e$ in Eq. (12) can be evaluated through a line integration along the element contour as

$$\boldsymbol{Q}_e = \int_{\Gamma_e} \boldsymbol{B}^T \boldsymbol{N}_\Gamma \boldsymbol{D} \, d\Gamma_e. \tag{13}$$

In addition, if $\boldsymbol{t}$ also satisfies internal compatibility equations, the matrix $\boldsymbol{H}_e$ of Eq. (12) can be evaluated by line integration along the element contour as well, thereby obtaining

$$\boldsymbol{H}_e = \int_{\Gamma_e} \boldsymbol{B}^T \boldsymbol{N}_\Gamma \boldsymbol{D}_t \, d\Gamma_e, \tag{14}$$

where $\boldsymbol{D}_t$ collects the shape functions for the elastic displacements $\boldsymbol{d}_t$ (see Eq. (9)) described in terms of stress interpolation parameters $\boldsymbol{t}_e$ as

$$\boldsymbol{d}_t = \boldsymbol{D}_t \boldsymbol{t}_e, \quad \begin{bmatrix} \boldsymbol{d}_{tm} \\ \boldsymbol{d}_{tf} \end{bmatrix} = \begin{bmatrix} \boldsymbol{D}_{tm} & \cdot \\ \cdot & \boldsymbol{D}_{tf} \end{bmatrix} \begin{bmatrix} \boldsymbol{\beta}_m \\ \boldsymbol{\beta}_f \end{bmatrix}. \tag{15}$$

3 MISS-4c LINEAR FORMULATION

3.1 Generalised stress field interpolation

The assumed interpolation for the generalised stresses is chosen so as to satisfy equilibrium equations for zero bulk loads and compatibility equations. Additionally, they are isostatic and then $n_\beta = 18$. The membrane and flexural generalised stress fields are interpolated separately and ruled by 9 static parameters each. Moreover, the generalised stresses are defined in the rotated local system $\{x, y, z\}$.

3.1.1 Assumed membrane stress field

To define the membrane stress field interpolation, a polynomial shape for the elastic displacement solution $\boldsymbol{d}_{tm}$ is assumed

$$\boldsymbol{d}_{tm} = \bar{\boldsymbol{B}}_m \bar{\boldsymbol{\beta}}_m \quad , \quad \bar{\boldsymbol{B}}_m = \begin{bmatrix} \bar{\boldsymbol{B}}_{mu} & \cdot \\ \cdot & \bar{\boldsymbol{B}}_{mu} \end{bmatrix}, \tag{16}$$

where

$$\bar{\boldsymbol{B}}_{mu} = \begin{bmatrix} 1 & x & y & x^2 & xy & y^2 & \dots & x^4 & x^3y & x^2y^2 & xy^3 & y^4 \end{bmatrix} \tag{17}$$

and $\bar{\boldsymbol{\beta}}_m$ is a $[30 \times 1]$ vector. By applying the compatibility and constitutive equations for the case of symmetric laminated composite to Eq. (16), the generalised membrane stresses become

$$\boldsymbol{t}_m = \boldsymbol{E}_m \boldsymbol{Q}_m \bar{\boldsymbol{B}}_m \bar{\boldsymbol{\beta}}_m. \tag{18}$$

Furthermore, the generalised membrane stresses can be rewritten by superimposing the equilibrium through Eq. (6). Afterwards, a hierarchical selection of 9 independent polynomials is conducted, leading to the interpolation explicitly given in [17]

Finally, the membrane part of the elastic displacement solution $\boldsymbol{d}_{tm}$ is expressed in terms of static parameters $\boldsymbol{\beta}_m$ as

$$\boldsymbol{d}_{tm} = \boldsymbol{D}_{tm} \boldsymbol{\beta}_m. \tag{19}$$

3.1.2 Assumed flexural stress field

To define the flexural stress field interpolation a polynomial shape for the elastic displacement solution $\boldsymbol{d}_{tf}$ is assumed

$$\boldsymbol{d}_{tf} = \bar{\boldsymbol{B}}_f \bar{\boldsymbol{\beta}}_f \quad , \quad \bar{\boldsymbol{B}}_f = \begin{bmatrix} \bar{\boldsymbol{B}}_{fu} & \cdot & \cdot \\ \cdot & \bar{\boldsymbol{B}}_{f\varphi} & \cdot \\ \cdot & \cdot & \bar{\boldsymbol{B}}_{f\varphi} \end{bmatrix} \tag{20}$$

with

$$\begin{aligned} \bar{\boldsymbol{B}}_{fu} &= \begin{bmatrix} 1 & x & y & x^2 & xy & y^2 & \cdots & x^5 & x^4y & x^3y^2 & x^2y^3 & xy^4 & y^5 \end{bmatrix}, \\ \bar{\boldsymbol{B}}_{f\varphi} &= \begin{bmatrix} 1 & x & y & x^2 & xy & y^2 & \cdots & x^4 & x^3y & x^2y^2 & xy^3 & y^4 \end{bmatrix} \end{aligned} \tag{21}$$

and where $\bar{\boldsymbol{\beta}}_f$ is a $[51 \times 1]$ vector. By applying the compatibility and constitutive equations for a symmetric laminated composite to eq. (20), the generalised flexural stresses the following expression

$$\boldsymbol{t}_f = \boldsymbol{E}_f \boldsymbol{Q}_f \bar{\boldsymbol{B}}_f \bar{\boldsymbol{\beta}}_f. \tag{22}$$

The generalised flexural stresses can be rewritten as explicitly shown in [17] by superimposing the equilibrium through Eq. (6) and after a hierarchical selection of 9 independent polynomials.

Finally, the flexural part of the elastic displacement solution $\boldsymbol{d}_{tf}$ is expressed in terms of static parameters $\boldsymbol{\beta}_f$ as

$$\boldsymbol{d}_{tf} = \boldsymbol{D}_{tf} \boldsymbol{\beta}_f. \tag{23}$$

3.2 Generalised displacement field interpolation

The interpolation of the displacement field $\boldsymbol{d}$ is ruled by 24 nodal translation and rotations, collected in the vector $\boldsymbol{d}_e$.

Due to the assumptions on the generalised stress field (see Section (3.1)), the displacement field is interpolated only along the contour of the FE. To this end, for a generic side Γ_k having end nodes i, j, the displacement parameters are collected in the vectors $\boldsymbol{d}_{ie} = [d_{ix},\, d_{iy},\, d_{iz},\, \varphi_{ix},\, \varphi_{iy},\, \varphi_{iz}]^T$ and $\boldsymbol{d}_{je} = [d_{jx},\, d_{jy},\, d_{jz},\, \varphi_{jx},\, \varphi_{jy},\, \varphi_{jz}]^T$, respectively.

3.3 Assumed membrane displacement field

The membrane displacements along the generic side Γ_k are defined as the sum of three contributions

$$\boldsymbol{d}_{km}[\zeta] = \boldsymbol{d}^{(l)}_{km}[\zeta] + \boldsymbol{d}^{(q)}_{km}[\zeta] + \boldsymbol{d}^{(c)}_{km}[\zeta], \tag{24a}$$

where ζ is the one-dimensional abscissa $-1 \leq \zeta \leq 1$ along Γ_k (see Eq. (**??**)). The first contribution in Eq. (24a) is a linear interpolation from the vertex values

$$\boldsymbol{d}^{(l)}_{km}[\zeta] = \frac{1}{2}[(1-\zeta)\,\boldsymbol{d}_i + (1+\zeta)\,\boldsymbol{d}_j]\,, \quad \boldsymbol{d}_i = [d_{ix},\, d_{iy}]^T\,, \quad \boldsymbol{d}_j = [d_{jx},\, d_{jy}]^T. \tag{24b}$$

The second contribution is a quadratic expansion for the normal displacement

$$\boldsymbol{d}^{(q)}_{km}[\zeta] = \frac{L_k}{8}\,(1-\zeta^2)(\varphi_{jz} - \varphi_{iz})\,\boldsymbol{n}_k \tag{24c}$$

evaluated according to Allman's kinematic [19]. Finally, the third contribution is a cubic expansion for the normal component of the side displacement defined as

$$\boldsymbol{d}_{km}^{(c)}[\zeta] = \frac{1}{4} L_k(\zeta - \zeta^3)\boldsymbol{n}_k \, \alpha_c, \tag{24d}$$

where α_c is the average distortional drilling nodal rotation obtained as

$$\alpha_c = \frac{1}{4}\sum_{i=1}^{4} \varphi_{iz} - \varphi_{ez}, \tag{24e}$$

where the expression of each term is given in [17]. The cubic contribution $\boldsymbol{d}_{km}^{(c)}[\zeta]$ is an incompatible mode introduced to avoid rank defectiveness, as discussed in [19].

3.4 Assumed flexural displacement field

The displacement $u_{kz}[\zeta]$ along Γ_k is assumed as the sum of a linear, a quadratic and a cubic contribution. The latter is introduced to avoid rank defectiveness. Their expressions are given in [17].

The normal rotation $\varphi_{kn}[\zeta]$ along Γ_k is assumed to be the sum of a linear and a quadratic contribution, while the tangential rotation $\varphi_{kt}[\zeta]$ is assumed to be linear.

4 GEOMETRICAL NONLINEAR FE BASED ON A COROTATIONAL APPROACH

A CR approach is used to transform the linear version of MISS-4c presented in Section 3 into a geometrically nonlinear FE [11, 10]. Within the fixed frame $\{\boldsymbol{e}_1, \boldsymbol{e}_2, \boldsymbol{e}_3\}$, a CR reference system $\{\bar{\boldsymbol{e}}_1, \bar{\boldsymbol{e}}_2, \bar{\boldsymbol{e}}_3\}$ is defined

$$\bar{\boldsymbol{e}}_k = \boldsymbol{R}_c[\boldsymbol{\alpha}]\boldsymbol{e}_k, \quad k = 1 \dots 3 \tag{25}$$

where $\boldsymbol{R}_c$ is a rigid rotation, parameterised through the rotation vector $\boldsymbol{\alpha}$ according to Rodrigues' formulation [25].

The origin of the CR frame is translated by the vector $\boldsymbol{c}$, while $\boldsymbol{d}$ and $\boldsymbol{R}$ denote displacements and rotations, respectively, at the position $\boldsymbol{X}$ in the fixed reference frame. The corresponding displacements and rotations in the CR frame, $\bar{\boldsymbol{d}}$ and $\bar{\boldsymbol{R}}$, are

$$\bar{\boldsymbol{d}} = \boldsymbol{R}_c^T(\boldsymbol{X} + \boldsymbol{d} - \boldsymbol{c}) - \boldsymbol{X} \quad , \quad \bar{\boldsymbol{R}} = \boldsymbol{R}_c^T\boldsymbol{R}. \tag{26}$$

Using a vector parameterisation for $\bar{\boldsymbol{R}}$ and $\boldsymbol{R}$ and denoting the rotation vectors by $\bar{\boldsymbol{\psi}}$ and $\boldsymbol{\psi}$, one has

$$\bar{\boldsymbol{\psi}} = \log(\bar{\boldsymbol{R}}[\bar{\boldsymbol{\psi}}]) = \log\left(\boldsymbol{R}_c^T[\boldsymbol{\alpha}]\boldsymbol{R}[\boldsymbol{\psi}]\right). \tag{27}$$

A CR frame can be defined for each element through the element rotation vector $\boldsymbol{\alpha}_e$ and the element origin $\boldsymbol{c}_e$, which are function of the element kinematical parameters $\boldsymbol{d}_e$ in the fixed frame, namely

$$\boldsymbol{\alpha}_e = \boldsymbol{\alpha}_e[\boldsymbol{d}_e] \quad , \quad \boldsymbol{c}_e = \boldsymbol{c}_e[\boldsymbol{d}_e] \tag{28}$$

The local kinematical parameters $\bar{\boldsymbol{d}}_e$ in the CR frame are related to $\boldsymbol{d}_e$ through the geometrical transformation

$$\bar{\boldsymbol{d}}_e = \boldsymbol{g}[\boldsymbol{d}_e] \tag{29}$$

where $\boldsymbol{g}$ collects the CR transformations for displacements and rotations, Eqs.(26) and (27), conveniently rearranged once the definition of local kinematic parameters $\bar{\boldsymbol{d}}_e$ is given.

Based on the relations given above, the linear FE characterised by the energy in Eq. (12) can be transformed into a geometrically nonlinear one by simply introducing a CR description and assuming that the elemental kinematical parameters in Eq. (12) are referred to the CR frame. Therefore, the FE energy can be expressed as

$$\Phi_e[\boldsymbol{t}_e, \boldsymbol{d}_e] = \boldsymbol{t}_e^T \boldsymbol{Q}_e \boldsymbol{g}[\boldsymbol{d}_e] - \frac{1}{2}\boldsymbol{t}_e^T \boldsymbol{H}_e \boldsymbol{t}_e. \tag{30}$$

The strain energy in each FE can be expressed in terms of the unknown vector

$$\boldsymbol{u}_e = \{\boldsymbol{t}_e,\, \boldsymbol{d}_e\}^T \tag{31}$$

which collects the parameters that define the configuration of a single FE. This vector can be related to the global configuration vector $\boldsymbol{u}$ through standard FE assemblage procedure

$$\boldsymbol{u}_e = \boldsymbol{A}_e \boldsymbol{u} \tag{32}$$

where the matrix $\boldsymbol{A}_e$ implicitly contains the connectivity constraints between elements.

5 Numerical results

The test regards a composite square plate under compression loading. Geometry, loads and boundary conditions are reported in Fig. 1. The length is $\ell = 0.508$, while the thickness is $1.172 \cdot 10^{-4}$. The plate is simply supported (SS1) and in-plane constraints are applied to remove rigid body motions. A compression load $q_x = 1$ is uniformly distributed along two end sides. Additionally, an out-of-plane uniformly distributed load $q_z = 10^{-8}$ is applied. A regular and a distorted mesh are considered, as shown in Fig. 1.

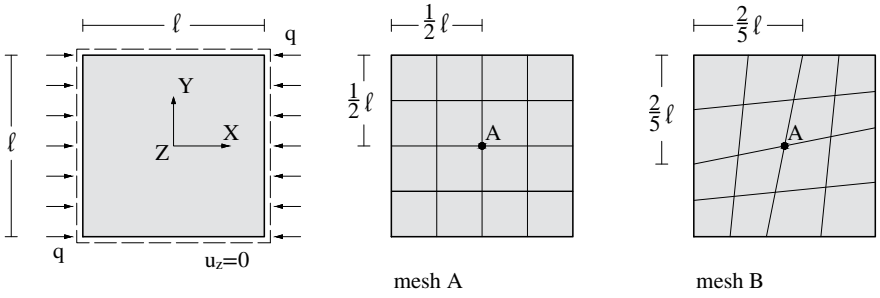

Figure 1: Composite plate: geometry, loads, boundary conditions and initial meshes.

The material properties are $E_{11} = 181 \cdot 10^3$, $E_{22} = 10.27 \cdot 10^3$, $G_{12} = 7.17 \cdot 10^3$, $G_{13} = G_{23} = 5.135 \cdot 10^6$ and $\nu_{12} = 0.28$. The material directions 1 and 2 are aligned along the directions x and y, respectively. The stacking sequence is $[\pm 45]_{2S}$.

Subsequently, the results of a linearised buckling analysis are presented. Figure 2 shows the convergence of the four lowest buckling loads for regular and distorted meshes of MISS-4 and

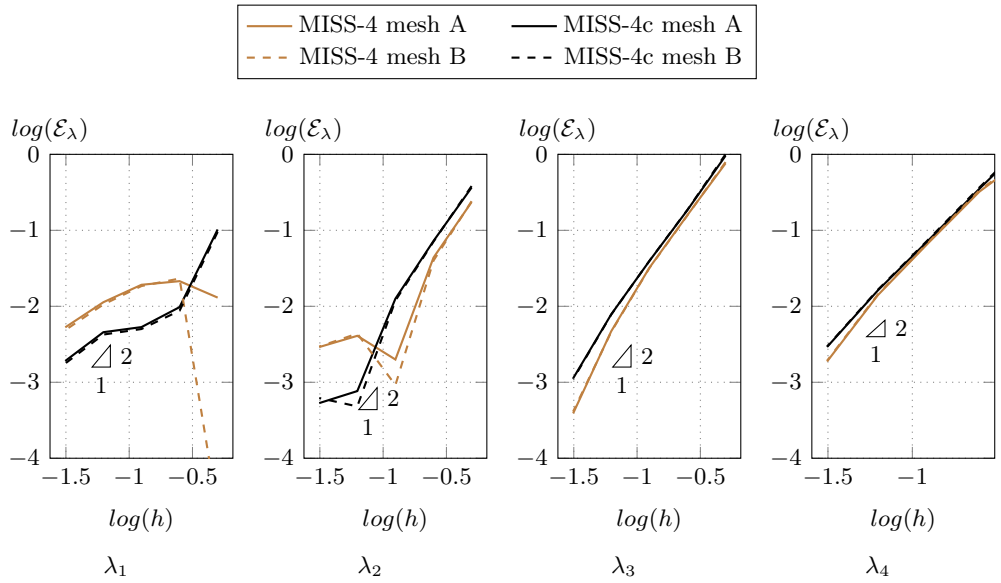

Figure 2: Composite plate: convergence of the four lowest buckling loads, lamination $[\pm 45]_{2s}$.

MISS-4. In all cases, a rate of convergence of h^2 is observed, while MISS-4c gives a lower error in the evaluation of the first buckling load.

The use of MISS-4c gives advantages over MISS-4 also in the evaluation of initial postbuckling response. This aspect can be observed in Fig. 3 that gives the equilibrium paths evaluated using MISS-4, MISS-4c and compared with a solution obtained with S8R and a path-following analysis. Only the first buckling mode is used in Koiter's analysis.

The influence of the stacking sequence on the accuracy of the proposed FE is studied. To this end, a parametric stacking sequence is introduced, namely $[0/90]_{2S} + \vartheta$, in which ϑ varies from 0° to 90°. Figure 4 shows the error in the evaluation of the first buckling load with varying ϑ and for different meshes and lower error for MISS-4c is observed in all cases.

REFERENCES

[1] D. J. Allman. A quadrilateral finite element including vertex rotations for plane elasticity analysis. *International Journal for Numerical Methods in Engineering*, 26(3):717–730, 1988.

[2] E.J. Barbero, A. Madeo, G. Zagari, R. Zinno, and G. Zucco. Koiter asymptotic analysis of folded laminated composite plates. *Composites Part B: Engineering*, 61:267 – 274, 2014.

[3] Federica Caselli and Paolo Bisegna. Polar decomposition based corotational framework for triangular shell elements with distributed loads. *International Journal for Numerical Methods in Engineering*, 95(6):499–528, 2013.

[4] Song Cen, Yan Shang, Chen-Feng Li, and Hong-Guang Li. Hybrid displacement function element method: a simple hybrid-trefftz stress element method for analysis of mindlin–reissner plate. *International Journal for Numerical Methods in Engineering*, 98(3):203–234, 2014.

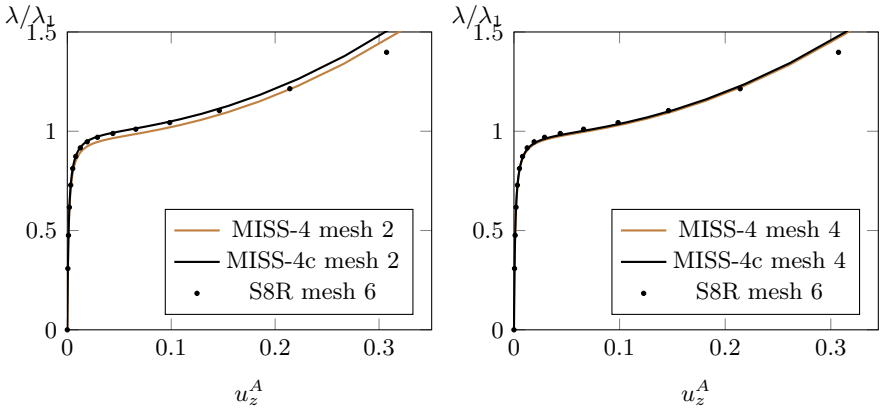

Figure 3: Composite plate: equilibrium path for the lamination $[\pm 45]_{2s}$, regular mesh and different levels of refinement.

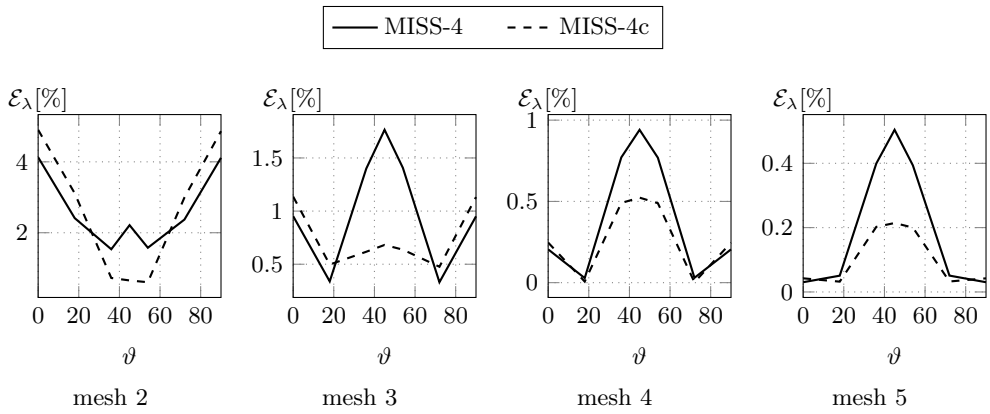

Figure 4: Composite plate: error in the evaluation of the first lowest buckling load for different mesh refinements for varying ϑ.

[5] Haeseong Cho, SangJoon Shin, and Jack J. Yoh. Geometrically nonlinear quadratic solid/solid-shell element based on consistent corotational approach for structural analysis under prescribed motion. *International Journal for Numerical Methods in Engineering*, 112(5):434–458, 2017.

[6] K.-S. Chun, S.K. Kassegne, and B.K. Wondimu. Hybrid/mixed assumed stress element for anisotropic laminated elliptical and parabolic shells. *Finite Elements in Analysis and Design*, 45(11):766–781, 2009. cited By 9.

[7] Stefano de Miranda and Francesco Ubertini. A simple hybrid stress element for shear deformable plates. *International Journal for Numerical Methods in Engineering*, 65(6):808–833, 2006.

[8] C.A. Felippa and B. Haugen. A unified formulation of small-strain corotational finite elements: I. theory. *Computer Methods in Applied Mechanics and Engineering*, 194(21):2285 – 2335, 2005. Computational Methods for Shells.

[9] G. Garcea, F. S. Liguori, L. Leonetti, D. Magisano, and A. Madeo. Accurate and efficient a posteriori account of geometrical imperfections in koiter finite element analysis. *International Journal for Numerical Methods in Engineering*, 112(9):1154–1174, 2017.

[10] G. Garcea, A. Madeo, and R. Casciaro. The implicit corotational method and its use in the derivation of nonlinear structural models for beams and plates. *Journal of Mechanics of Materials and Structures*, 7(6):509–539, 2012.

[11] G. Garcea, A. Madeo, G. Zagari, and R. Casciaro. Asymptotic post-buckling FEM analysis using corotational formulation. *International Journal of Solids and Structures*, 46(2):377–397, 2009.

[12] Andrea Genoese, Alessandra Genoese, Antonio Bilotta, and Giovanni Garcea. A geometrically exact beam model with non-uniform warping coherently derived from the saint venant rod. *Engineering Structures*, 68:33 – 46, 2014.

[13] Eisuke Kita and Norio Kamiya. Trefftz method: an overview. *Advances in Engineering Software*, 24(1):3 – 12, 1995.

[14] W.T. Koiter. *On the stability of elastic equilibrium*. Techische Hooge School at Delft, english transl. nasa tt-f10, 883 (1967) and affdl-tr70-25 (1970) edition, 1945.

[15] Leonardo Leonetti, Francesco S. Liguori, Domenico Magisano, Josef Kiendl, Alessandro Reali, and Giovanni Garcea. A robust penalty coupling of non-matching isogeometric kirchhoff–love shell patches in large deformations. *Computer Methods in Applied Mechanics and Engineering*, 371:113289, 2020.

[16] Leonardo Leonetti, Domenico Magisano, Francesco Liguori, and Giovanni Garcea. An isogeometric formulation of the koiter's theory for buckling and initial post-buckling analysis of composite shells. *Computer Methods in Applied Mechanics and Engineering*, 337:387 – 410, 2018.

[17] Francesco S. Liguori and Antonio Madeo. A corotational mixed flat shell finite element for the efficient geometrically nonlinear analysis of laminated composite structures. *International Journal for Numerical Methods in Engineering*, 122(17):4575–4608, 2021.

[18] Francesco S. Liguori, Giovanni Zucco, Antonio Madeo, Giovanni Garcea, Leonardo Leonetti, and Paul M. Weaver. An isogeometric framework for the optimal design of variable stiffness shells undergoing large deformations. *International Journal of Solids and Structures*, 2020.

[19] A. Madeo, G. Zagari, and R. Casciaro. An isostatic quadrilateral membrane finite element with drilling rotations and no spurious modes. *Finite Elements in Analysis and Design*, 50:21–32, 2012.

[20] A. Madeo, G. Zagari, R. Casciaro, and S. De Miranda. A mixed 4-node 3d plate element based on self-equilibrated isostatic stresses. *International Journal of Structural Stability and Dynamics*, 15(4), 2015.

[21] Antonio Madeo, Francesco S. Liguori, Giovanni Zucco, and Stefania Fiore. An efficient isostatic mixed shell element for coarse mesh solution. *International Journal for Numerical Methods in Engineering*, n/a(n/a).

[22] M. Mostafa. An improved solid-shell element based on ans and eas concepts. *International Journal for Numerical Methods in Engineering*, 108(11):1362–1380, 2016.

[23] Daniel Peeters, Daniel van Baalen, and Mostafa Abdallah. Combining topology and lamination parameter optimisation. *Structural and Multidisciplinary Optimization*, 52:105–120, 2015.

[24] C.C. Rankin and B. Nour-Omid. The use of projectors to improve finite element performance. *Computers and Structures*, 30(1):257 – 267, 1988.

[25] M. Ritto-Corrêa and D. Camotim. On the differentiation of the rodrigues formula and its significance for the vector-like parameterization of reissner–simo beam theory. *International Journal for Numerical Methods in Engineering*, 55(9):1005–1032, 2002.

[26] A.W. Ruggerini, A. Madeo, R. Gonçalves, D. Camotim, F. Ubertini, and S. de Miranda. Gbt post-buckling analysis based on the implicit corotational method. *International Journal of Solids and Structures*, 163:40 – 60, 2019.